

Low Voltage Asymmetrical Half-Bridge Converter with Integrated Magnetics

H. Wetzel¹, A. Siegel², H. D. Njiende¹, N. Fröhleke¹, J. Böcker¹

¹Institute of Power Electronics and Electrical Drives, University of Paderborn

Warburger Str. 100, Paderborn, Germany

²Paragon sensors + systems AG

Schwalbenweg 29, Delbrück, Germany

¹Phone +49 5251 60 3653 Fax +49 5251 60 3443 E-Mail: wetzel@lea.upb.de WWW: <http://www.lea.upb.de>

²WWW: <http://www.paragon-online.de>

Abstract - An Asymmetrical Half Bridge Converter (AHBC) with integrated magnetic components is presented in this contribution. After describing the circuit function, the design of an integrated magnetic current doubler component is discussed, supplemented by the derivation of an advanced average model of the AHBC. A prototype of the AHBC is built for a low voltage application of 1.7V rated output voltage at 20A rated output current, which represents the base for validation of theoretical results.

I. INTRODUCTION

Modern computers, automation equipment and telecommunication systems require highly dynamically controlled low voltage DC/DC converters at output voltages of 1 and 2 Volt, which even fall below one Volt in the near future. If the rating of the supplying input voltages range about 48 Volt, only insulated converters qualify for this target application¹ [1].

Miscellaneous topologies are offered in literature to be used in the low voltage field [2], [3], [5]. The pallet of these solutions is very wide and ranges from simple Two Transistor Forward Converter (2TFC) and Active Clamped Forward Converter (ACFC) to elaborate Push-Pull Converter (PPC) and bridge topologies. The asymmetrical driven Half Bridge Converter (AHBC) discussed in this contribution (see Fig. 1) combines the advantages of bridge topologies and simplicity of forward converters. On recent conferences half bridges were addressed in conjunction with the low voltage topic several times, e.g. in [4]. Using the Full Bridge Topology for low voltage converters at low power levels would be uneconomical from cost reasons. The asymmetrical driving permits zero-voltage switching (ZVS) and reduces primary sided switching losses in the AHBC. Utilization of the synchronous rectification in conjunction with the current doubler scheme reduces secondary sided forward losses noticeable. Low voltage stress of primary sided MOSFETs, good utilization of transformer core and continuous energy flow are the advantages of AHBC. Furthermore, a transformer winding ratio smaller than for other forward converters and bridges can be selected, reducing the core volume and the winding complexity, while the current stress is doubled. The asymmetrical stress of all components is the main disadvantage of AHBC. This problem complicates the

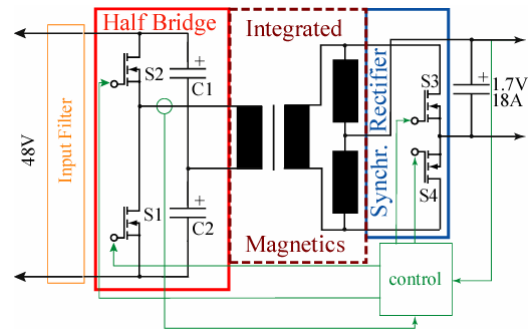


Fig. 1. Asymmetrical Half Bridge converter with integrated magnetics and synchronous rectification

choice of semiconductors and design of integrated magnetics. The modeling and control design of AHBC is intricate, because of a nonlinear transfer ratio.

II. CIRCUIT DESCRIPTION

The biggest and most costly elements in the circuit are the main transformer and the filter inductors. The integration of both magnetic components on one core approves clearly volume reduction and brings extra advantages. In order to clarify gains of magnetic integration the components were designed and built first in discrete and followed in integrated form (s. Fig. 2). This contribution focuses only on the integrated part of this parallel design, since discrete components are well known in literature. Furthermore the intermediate steps from Fig. 2a to Fig. 2b are assumed as known ([2], [4]) and are omitted for brevity.

The duty ratio for the AHBC (Fig. 1) with integrated magnetic (Fig. 2b) is calculated as:

$$D = 0.5 - \sqrt{0.25 - \frac{V_{out}}{V_{in}} \frac{n_{prim\Sigma}}{n_{sec\Sigma}}}, \text{ with } n_{prim\Sigma} = n_{p1} + n_{p2}$$

$$\text{and } n_{sec\Sigma} = n_{s1} + n_{s2},$$

which are the total winding turns of the primary and secondary side of the integrated transformer. This nonlinear control law is valid for $D \leq 0.5$; it can also be mirrored for $D > 0.5$ theoretically. Practically the unique operating area of the prototype circuit points are limited to $D \leq 0.5$.

A crucial drawback of the AHBC using symmetrical magnetics is the asymmetrical allocation of both partial

¹ Within named in the acknowledgement project www.sfb614.de the investigated circuit using an optimized integrated magnetic concept is planned as auxiliary power supply with largely shrunk volume and weight in order to be placed on the rail shuttle.

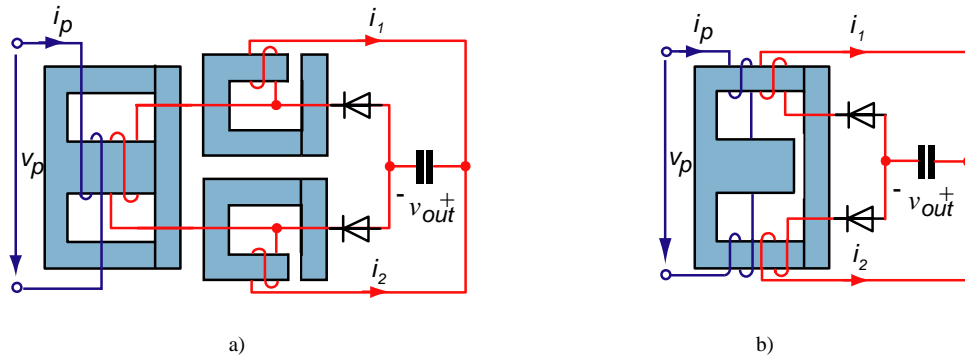


Fig. 2. Magnetics of the AHBC
a) discrete; b) integrated

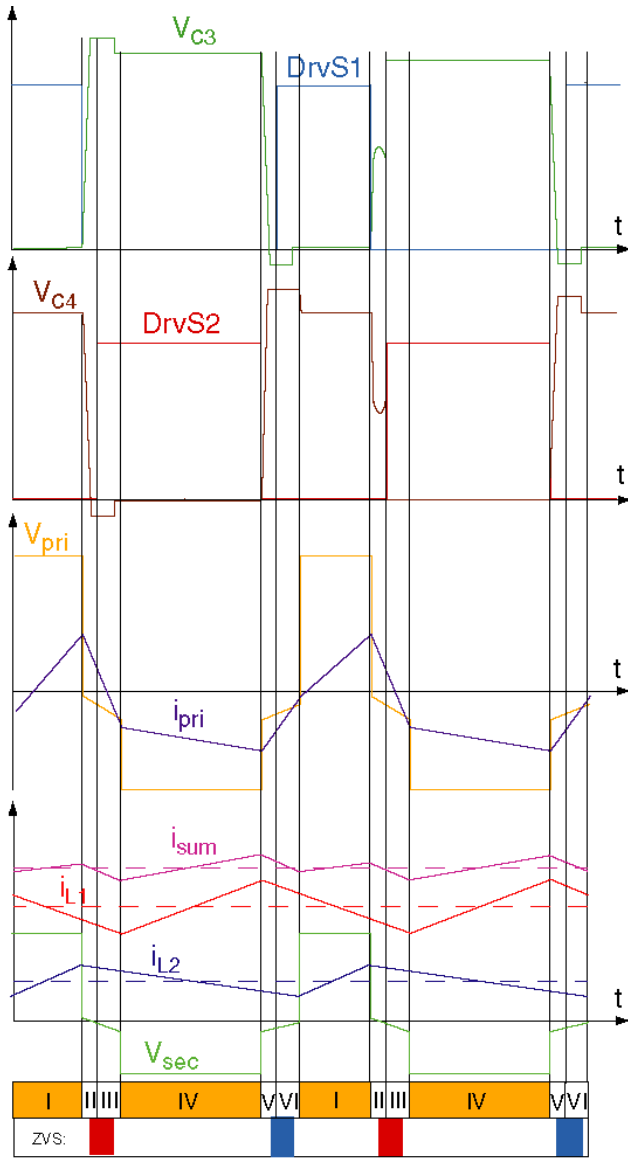


Fig. 3. Principal waveforms and intervals of the AHBC

output currents i_1 and i_2 . The correlation between average values of both currents can be calculated as

$$I_2 D = I_1 (1 - D).$$

Usually the AHBC is designed so that the rated duty cycle amounts to $D=0.3 \dots 0.4$. In case of $D=0.3$ the current I_2 is twice that of I_1 . This problem must be considered at the design stage of the magnetics and when selecting the semiconductors. Thus, a possible solution is by applying an asymmetrical magnetic component. But real advantages of asymmetrical magnetics should be analyzed critically because of volume, cost and feasibility. This topic will be addressed in a future publication.

Fig. 3 shows principal voltage and current waveforms of AHBC. During the main intervals I and IV, transistors S1 and S2 are conducting accordingly and the energy is being transferred from input to output of the AHBC. The switching transients between these main states are performed in commutation intervals II, III and V, VI, whereby each interval II, III and V, VI, resp., consists of two single commutations. During these commutations, a zero voltage switching of S1 and S2 can be realized. Fig. 3 shows a "true" ZVS during the first occurrence of intervals II and III, and next time of II and III an soft switching. Due to the asymmetrical distribution of the partial output currents, the ZVS can occur only at one of both commutations, so that one of the primary sided switches is charged more than the other.

Simulations and measurements at the prototype of the AHBC have shown the critical sensitivity of this topology to exact timing of the driving signals of all semiconductors.

For the realization of the ZVS two general strategies can be chosen. The general solution is the detection of the literal Zero Voltage at S1 and S2. But since S1 and S2 do not share a common ground, this measure is cardinaly possible, but relatively complicated. Besides in isolated converters the control and driving is placed mostly at the secondary side of the main transformer [5]. Therefore this solution was not realized for the prototype for low cost applications.

Other "basic" alternatives operate with fixed delays between both driving signals $DrvS1$ and $DrvS2$ (intervals II and V). These delays should be selected so that on the one hand ZVS is enabled in a relevant operation range preferably at higher currents, and on the other hand these delays must be obviously smaller as the conduction intervals.

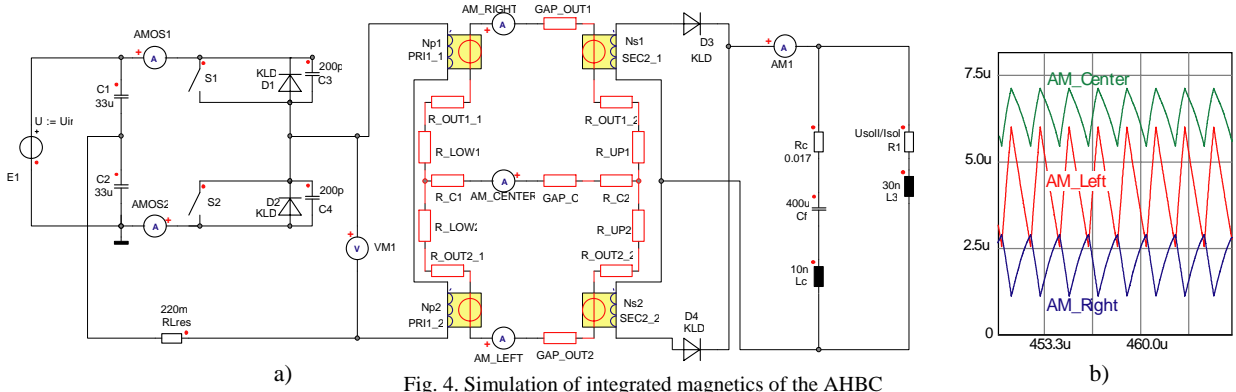


Fig. 4. Simulation of integrated magnetics of the AHBC
a) SIMLORER-sheet; b) time behavior of magnetic fluxes

III. INTEGRATED MAGNETICS

The functionality and the design of integrated magnetics are discussed by several authors and contributions [2], [3], [4], [9] and [10]. The core of this design is the inductance matrix L , where the diagonal elements present the self inductances and the off-diagonals the mutually coupled inductances of the integrated magnetic component:

$$L = \begin{bmatrix} \frac{n_{p2}^2 R_1 + n_{p1}^2 R_2 + n_{p1}^2 R_C + 2n_{p1}n_{p2}R_C + n_{p2}^2 R_C}{R_1 R_2 + R_1 R_C + R_2 R_C} & \frac{n_{s1}(n_{p1}R_2 + n_{p1}R_C + n_{p2}R_C)}{R_1 R_2 + R_1 R_C + R_2 R_C} & \frac{n_{s2}(n_{p2}R_1 + n_{p1}R_C + n_{p2}R_C)}{R_1 R_2 + R_1 R_C + R_2 R_C} \\ \frac{n_{s1}(n_{p1}R_2 + n_{p1}R_C + n_{p2}R_C)}{R_1 R_2 + R_1 R_C + R_2 R_C} & \frac{n_{s1}^2 (R_2 + R_C)}{R_1 R_2 + R_1 R_C + R_2 R_C} & \frac{n_{s1}n_{s1}R_C}{R_1 R_2 + R_1 R_C + R_2 R_C} \\ \frac{n_{s2}(n_{p2}R_1 + n_{p1}R_C + n_{p2}R_C)}{R_1 R_2 + R_1 R_C + R_2 R_C} & \frac{n_{s1}n_{s1}R_C}{R_1 R_2 + R_1 R_C + R_2 R_C} & \frac{n_{s2}^2 (R_1 + R_C)}{R_1 R_2 + R_1 R_C + R_2 R_C} \end{bmatrix}$$

According to this inductance matrix, a SIMPLORER model of this integrated component was realized using magnetic bibliotheca of this simulation tool. Fig. 4a shows the reluctance model of integrated magnetics as core of the

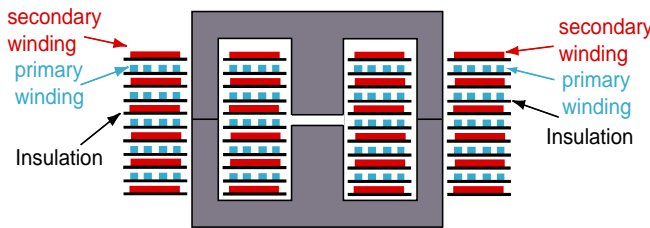


Fig. 5. Construction of integrated magnetic component

complete simulation sheet. Magnetic fluxes in the respective leg are displayed separately in Fig. 4b. The asymmetrical flux distribution between left and right leg is

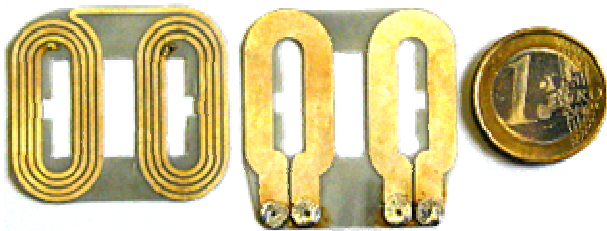


Fig. 6. Primary and secondary windings of integrated magnetics

easily visible. Due to ripple cancellation through a special winding orientation [2], [3], a relatively small ripple of the magnetical flux results in the center leg.

The integrated magnetic component was built using multilayer planar technique. Fig. 6 shows the construction of this component. Because of reduction of leakage inductance primary and secondary windings were interleaved. In order to facilitate fast configuration

changes primary and secondary windings were manufactured separately using skin one-sided PCBs (s. Fig. 6). For industrial applications all windings will be realized using multilayer PCB. Thereby coupling between primary and secondary side will be higher, so that leakage inductances are reduced. Besides the total volume will be reduced and an EI-core combination instead of EE can be used.

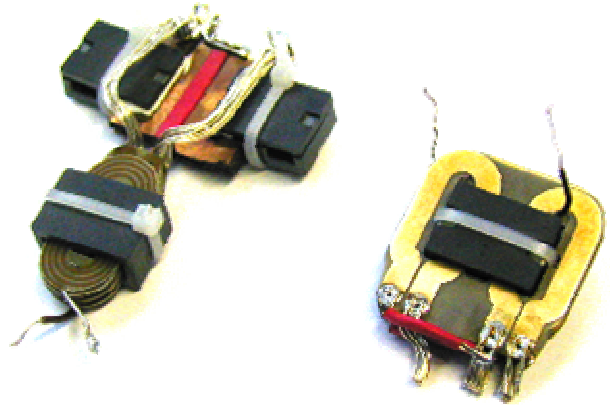


Fig. 7. Separate transformer and inductors versus integrated magnetic component

In the framework of diploma thesis [6] the current doubler circuit was built first by using separate coils, followed by their integration to one component (s. Fig. 7). Besides higher conduction losses due to a higher number of nodes, the circuit with separate coils reveals articulate larger leakage inductances so that the comparison of both solutions is only conditionally possible. Construction volume alone exhibits the advantages of integrated magnetic component. Reduction of cost, losses and other parasitic effects make using of integrated components inevitable in the future.

IV. SYSTEM MODELING

For the modeling of the AHBC an advanced average model was derived based on [8] considering not only the main but also the commutation intervals. State, input and output variables, as well as system and input matrices can be calculated as:

$$\hat{x}(t) = \begin{bmatrix} \hat{v}_{C1}(t) \\ \hat{v}_{C2}(t) \\ \hat{i}_m(t) \\ \hat{i}_{L1}(t) \\ \hat{i}_{L2}(t) \\ \hat{v}_{Cout}(t) \end{bmatrix} \quad \hat{u}(t) = \begin{bmatrix} \hat{v}_m(t) \\ \hat{i}_2(t) \end{bmatrix}$$

$$\hat{y}(t) = \hat{v}_{out}(t)$$

$$A_g = A_1 D_{cor1} + A_2 D_{cor3} + A_3 D_{cor3} + A_4 D_{cor4}$$

$$B_g = B_1 D_{cor1} + B_2 D_{cor3} + B_3 D_{cor3} + B_4 D_{cor4}$$

The corresponding differential equations result from the following system definition:

$$\frac{d\hat{x}(t)}{dt} = A_g \hat{x}(t) + (A_1 \hat{d}_1(t) + A_2 \hat{d}_2(t) + A_3 \hat{d}_3(t) + A_4 \hat{d}_4(t)) X_{cor}$$

$$+ (B_1 \hat{d}_1(t) + B_2 \hat{d}_2(t) + B_3 \hat{d}_3(t) + B_4 \hat{d}_4(t)) U + B_g \hat{u}(t)$$

$$\hat{y}(t) = c_{cor}^T \hat{x}(t) + f_{cor}^T \hat{u}(t)$$

The control transfer function (duty ratio to output voltage) results as:

$$G_d(s) = \frac{\hat{v}_{out}(s)}{\hat{d}(s)} = c_{cor}^T (sE - A_g)^{-1} ((A_2 - A_4) X_{cor} + (B_2 - B_4) U)$$

If the commutation intervals are noticeable smaller as main intervals a simplified model using classical average modeling method can be adopt. Anymore the model order can be reduced from 6 to 4. Thereby capacitor voltages v_{C1} and v_{C2} can be pooled and transformer magnetizing current i_m can be allowed in both inductor currents i_{L1} and i_{L2} .

Fig. 8 shows theoretical and measured frequency responses of transfer function $G_d(s)$. Both curves exhibit a good concordance. Minor differences in damping are to be explained by imprecise statement of losses of simplified model.

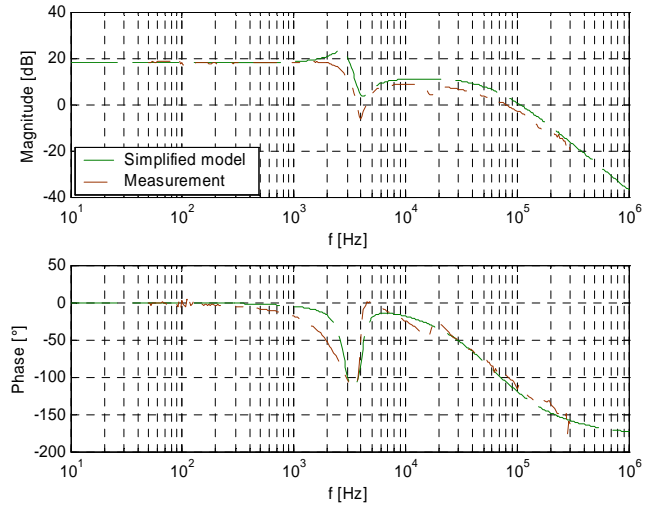


Fig. 8. Frequency responses of $G_d(s)$

V. PROTOTYPING AND MEASUREMENTS

A prototype circuit of AHBC was built to verify the theoretical results.

Fig. 9 shows the efficiency of AHBC including all driving and control losses.

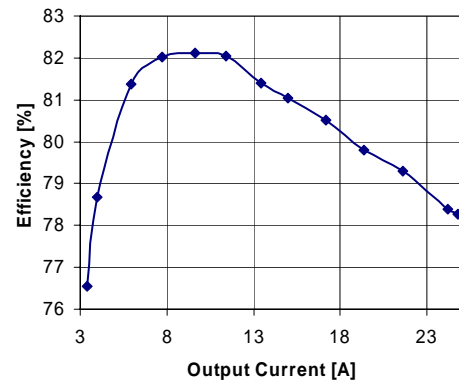


Fig. 9. Efficiency of AHBC at 40V input voltage and 400kHz switching frequency

VI. SUMMARY AND OUTLOOK

An Asymmetrical Half Bridge Converter is discussed in this contribution. Integrated magnetics used in this converter for best performance, weight, volume and cost reduction was designed and built using planar technique. An advanced average model and a simplified average model are given for the AHBC for deriving the open loop frequency responses.

ACKNOWLEDGMENT

This work was partly developed in the course of the Collaborative Research Center 614 - Self-Optimizing Concepts and Structures in Mechanical Engineering - University of Paderborn, and was published on its behalf and funded by the Deutsche Forschungsgemeinschaft.

Hermann Wetzel thanks Dietmar Kaberow [7] for supporting of system modeling of the AHBC.

REFERENCES

- [1] Basile Margaritis, Peter Ide, "Contemporary Architectures for Power System Considering Future Trends," *Proceedings of the 23rd IEEE International Telecommunications Energy Conference (Intelec)*, Edinburgh, UK, 14-18 Oct. 2001.
- [2] Peng Xu, Fred C. Lee, "Design of High-Input Voltage Regulator Modules With A Novel Integrated Magnetics," *IEEE Applied Power Electronics Conf. Proc. (APEC)*, Anaheim 2001, pp. 262-267.
- [3] Peng Xu, Jia Wei, Fred C. Lee, "The Active-Clamp Couple-Buck Converter - A Novel High Efficiency Voltage Regulator Modules," *IEEE Applied Power Electronics Conf. Proc. (APEC)*, Anaheim 2001, pp. 252-257.
- [4] Jian Sun, Vivek Mehrotra, "Unified Analysis of Half-Bridge Converters with Current-Doubler Rectifier." *IEEE Applied Power Electronics Conf. Proc. (APEC)*, Anaheim 2001, pp. 514-520.
- [5] Hermann Wetzel, Norbert Fröhleke, Peter Ide, Franz Meier, "Comparison of Low Voltage Topologies for Voltage Regulator Modules," *IEEE Industry Applications Society Proc. (IAS)*, October 2002, Pittsburgh, Pennsylvania, USA, Vol.2, pp. 1323-1329.
- [6] Andrei Siegel, "Halbbrücken-Schaltung mit integrierten magnetischen Komponenten für Stromversorgungen geringer Ausgangsspannung," *Diploma thesis, University of Paderborn*, 2003.
- [7] Dietmar Kaberow, "Regelungstechnische Aspekte bei Stromversorgungen geringer Ausgangsspannung," *Diploma thesis, University of Paderborn*, 2003.
- [8] Basile Margaritis, „Analyse des Sperr-Flußkonverters,“ *Dissertation Thesis D14-33, Univ. of Paderborn*, 1989
- [9] H. Njiende, H. Wetzel, N. Fröhleke, W. A. Cronje, „Models of Integrated Magnetic Components for Simulation Based Design of SMPS with SIMPLORER,“ *10th European Conference on Power Electronics and Applications (EPE 2003)*, September 2-4, 2003, Toulouse, France.
- [10] H. Njiende, N. Fröhleke, W. A. Cronje, "Modeling and Analysis of Integrated Magnetic Components," *IEEE Power Electronics Specialists Conference (PESC'03)*, 2003, Acapulco, Mexico, pp. 283-288.